SUPPLEMENTAL FIGURES

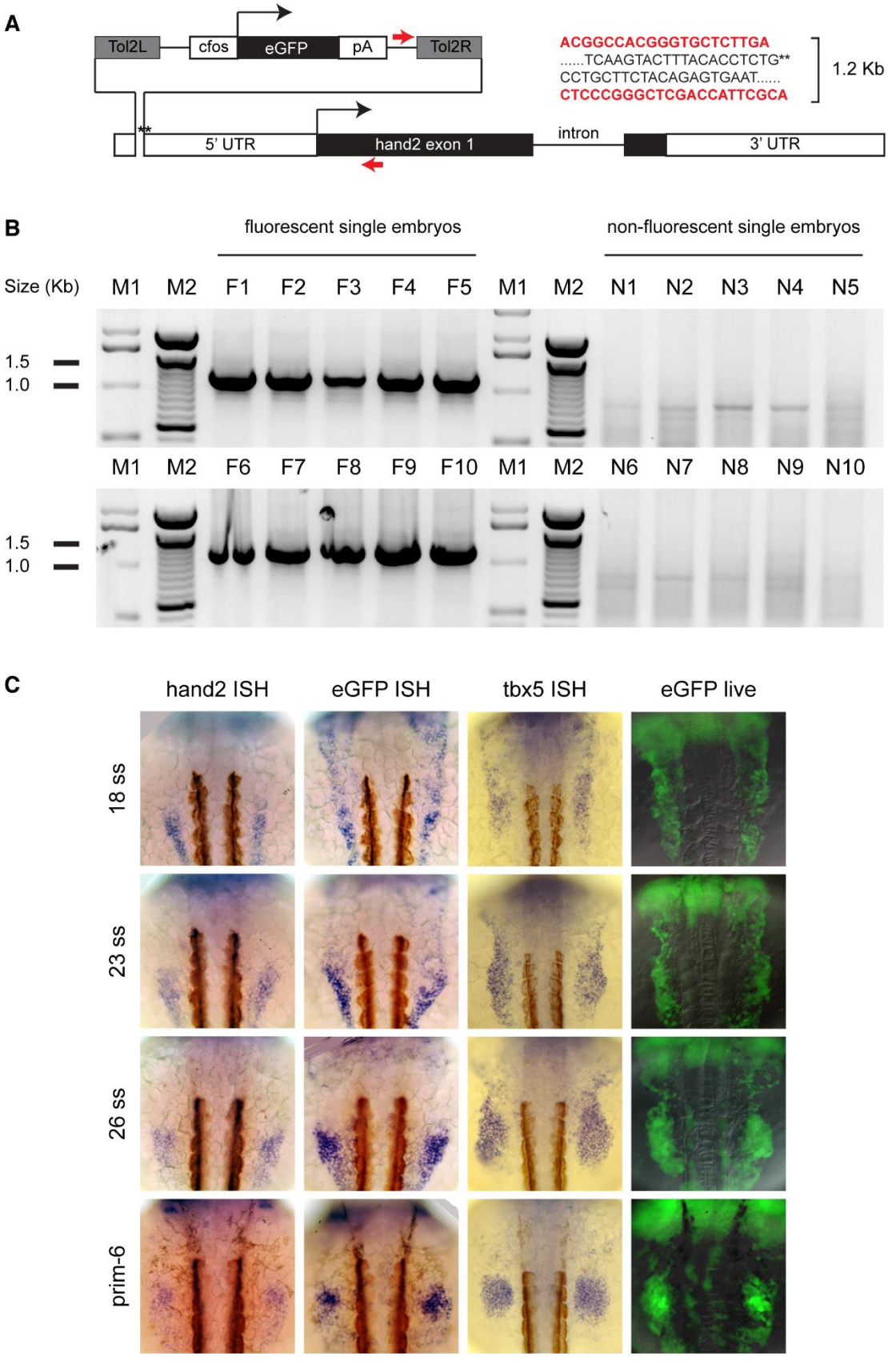

Figure S1. Et(hand2:eGFP)ch2 is a hand2 enhancer-trap line
A) Location and structure of the Tol2 transposon in *hand2* 5'-UTR. Paired red arrows show primers for the genotyping PCR and correspond to sequences highlighted in red.
B) Single-embryo genotyping PCR shows presence of 1.2 kb band in 10 embryos with hand2:eGFP fluorescence and a lack thereof in 10 non-fluorescent siblings.
C) Expression patterns of *hand2* mRNA, *egfp* mRNA, *tbx5* mRNA and eGFP protein in the pectoral limb field during limb bud initiation. Note the resemblance between *hand2* mRNA and *egfp* mRNA expression patterns, as well as that between *tbx5* mRNA and eGFP protein expression patterns. Dorsal view, anterior up.

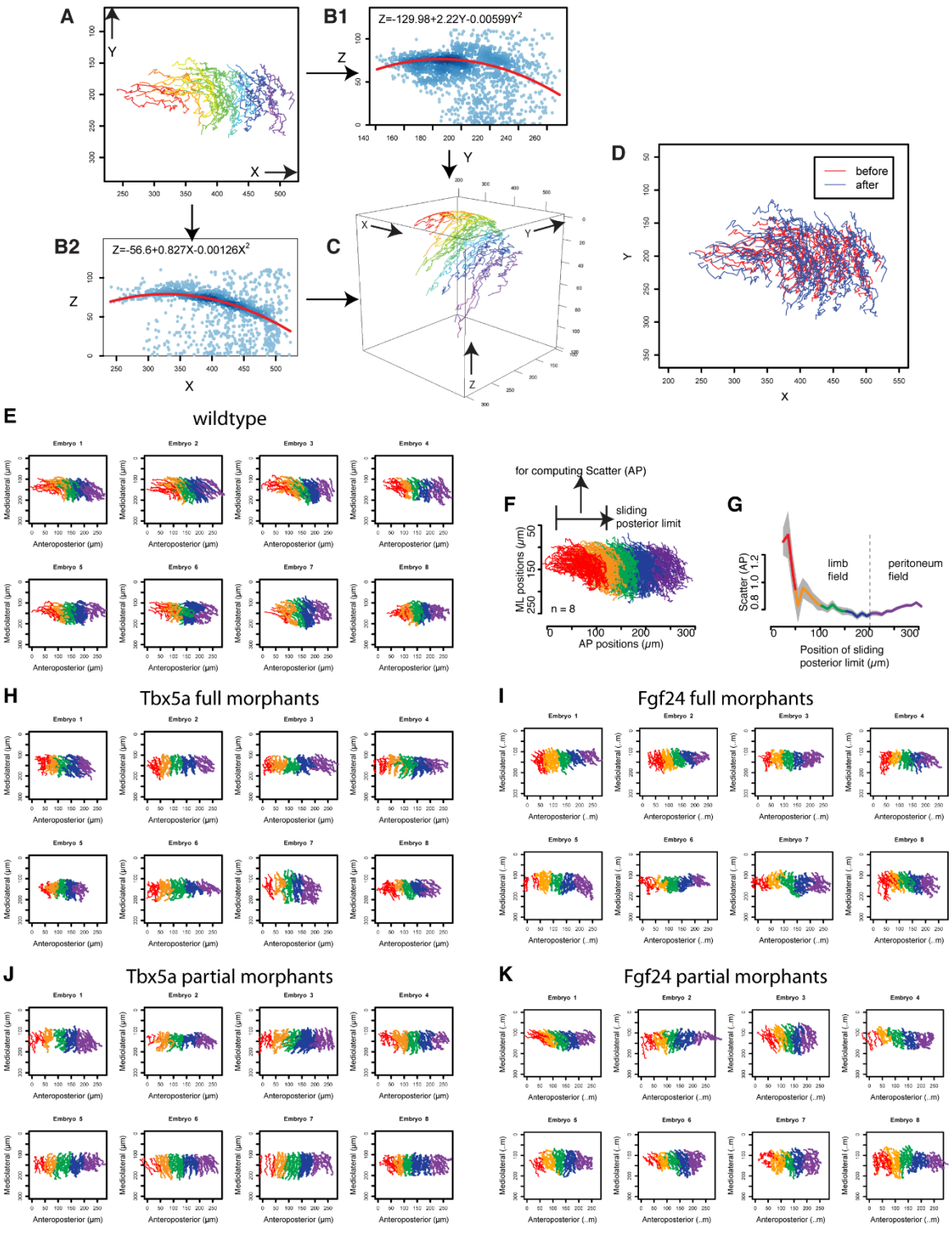

Figure S2. (related to Figure 2, 3, 4). A semi-automatic 4D cell tracking procedure
A) 2D cell tracks with (X, Y) coordinates are generated from the maximum intensity projection of confocal Z-stacks with the FIJI Manual Tracking plugin.
B1, B2) The Z coordinate for each (X, Y) is retrieved from the original Z-stacks by a custom automatic tracking ImageJ macro. A parabolic regression line is then fitted to entire sets of (X,Z) or (Y,Z) coordinates with a noise-resistant regression procedure (Rousseeuw and Leroy, 2005).
C) Reconstructed 3D tracks shown in (X, Y, Z).
D) Comparison between the original (X,Y) tracks (red) with the flattened (X, Y) tracks converted from the 3D tracks in C) (blue) following the Digital Flat Mount procedure.
E, H-K) shows cell tracks from individual embryos of 8 wildtype E), 8 Tbx5a full morphants H), 8 Fgf24 full morphants I), 8 Tbx5a partial morphants J), and 8 Fgf24 partial morphants K). Tracks are color-coded according to the somite level at which the track originated: red, orange, green, blue, and purple represent somite levels 1, 2, 3, 4, 5 and more posterior, respectively.
F) In the wildtype dataset, a group of cell tracks between a constant anterior limit and a sliding posterior limit are used to compute the Scatter value along the AP axis. Color code follows E).
G) The AP Scatter value plotted against the position of the sliding posterior limit used compute that AP Scatter value. Dashed line in B indicates the position of lowest AP Scatter value. Color code follows E).

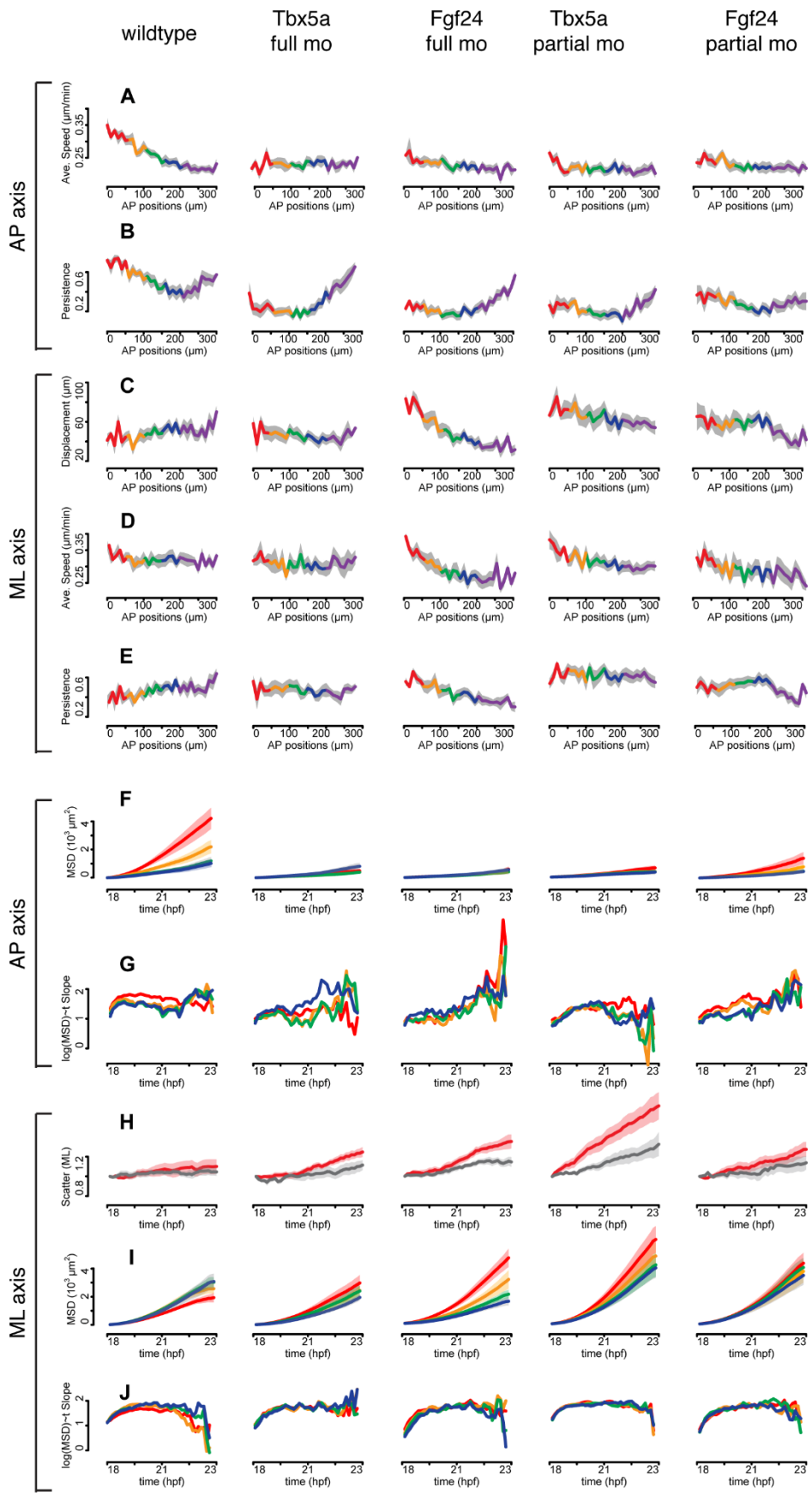

Figure S3 (related to Figures 2, 3, and 4). Additional motility parameters of limb field cells along the AP and ML axes in wildtype, Tbx5a full morphants, Fgf24 full morphants, Tbx5a partial morphants and Fgf24 partial morphants

Row A): Average AP speed plotted against the AP axis.
Row B): AP Persistence plotted against the AP axis.
Row C): Displacement along the mediolateral axis (ML) plotted against the AP axis.
Row D): Average ML speed plotted against the AP axis.
Row E): ML Persistence plotted against the AP axis.
Row F): AP Mean Squared Displacement (MSD_AP) plotted against time.
Row G): Slope of log(MSD_AP) plotted against time.
Row H): Scatter along the ML axis plotted against time.
Row I): MSD along the ML axis (MSD_ML) plotted against time.
Row J): Slope of log(MSD_ML)~t plotted against time.
Color code follows that in Figure S2E.

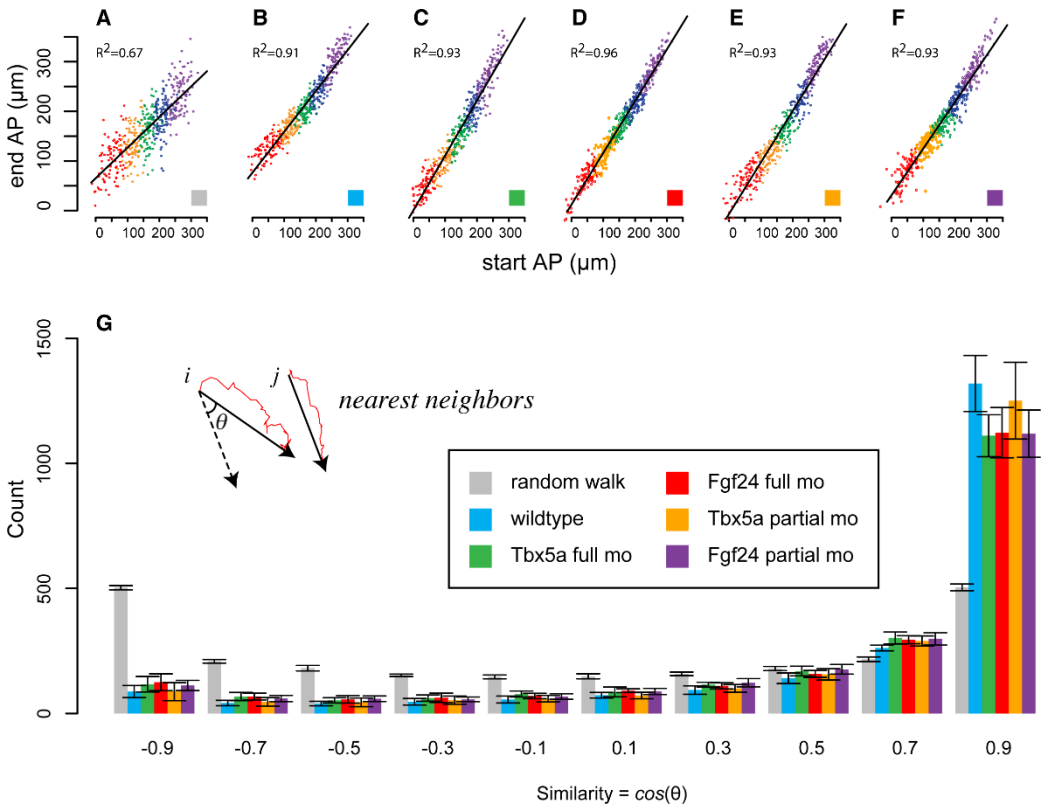

Figure S4 (related to Figures 2 and 3). Spatiotopic migration of limb field cells is correlated with a constraint on motility angles between nearest neighbors

A~F) Correlation between the start and the end AP positions of LPM cell tracks in wildtype B), Tbx5a full morphants C), Fgf24 full morphants D), Tbx5a partial morphants E), Fgf24 partial morphants F), and from a simulated 2D random walking group A). R^2 is the coefficient of determination.

G) Histogram of Similarity of nearest neighbors in wildtype, Tbx5a full morphants, Fgf24 full morphants, Tbx5a partial morphants, Fgf24 partial morphants, and from a simulated 2D random walk. Error bars indicate the 8-embryo standard error. i and j are in the schema are two nearest neighbors.

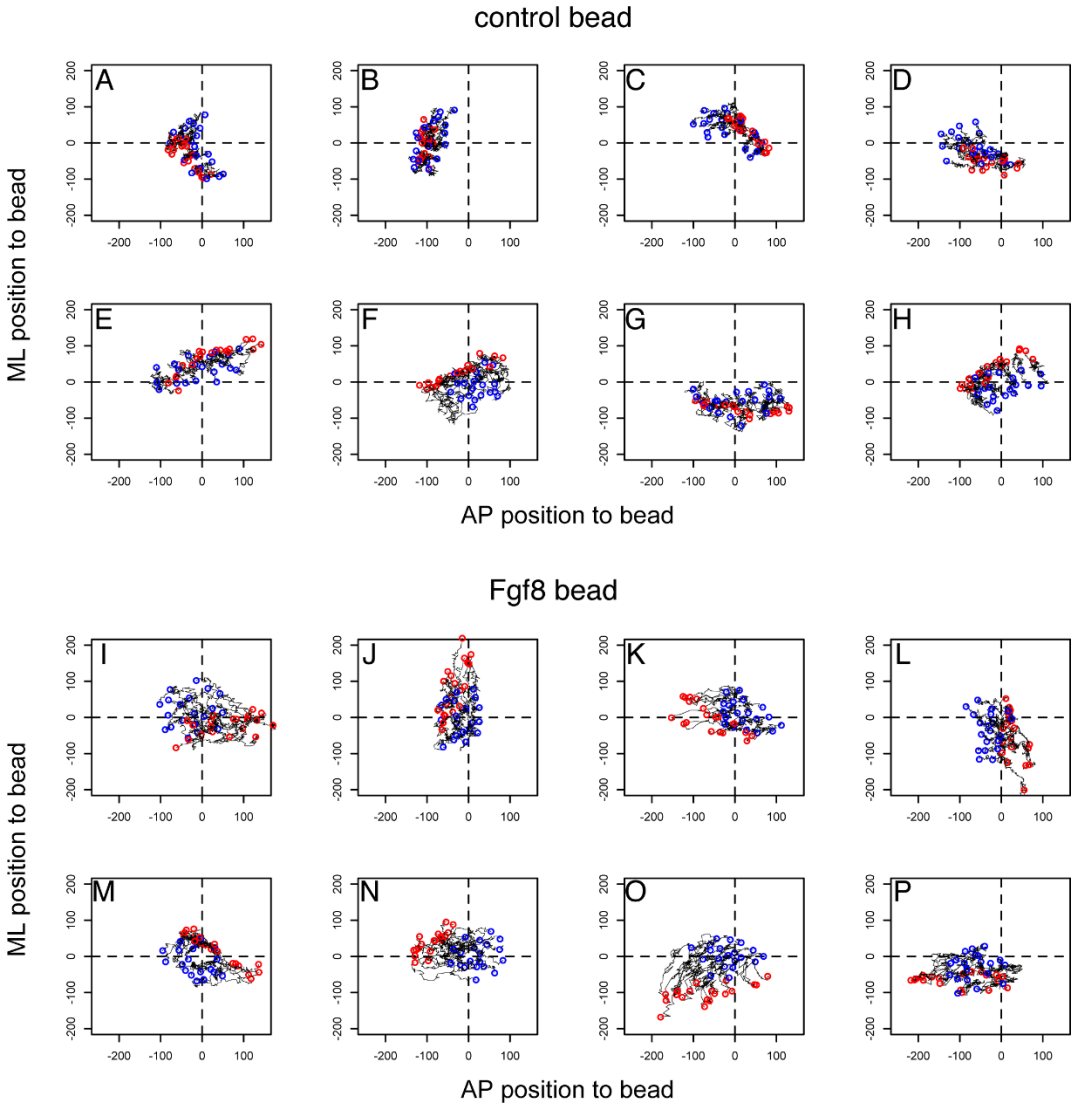

Figure S5 (related to Figure 5). LPM cell tracks in bead-implanted Fgf24 morphant embryos.
Circles highlight start (red) and end (blue) positions of each cell track in control bead (A-H) and Fgf8-coated bead (I-P) implanted embryos (n=20 cells per embryo). Units in each axis are in pixels (pixel size 0.8 μm in X and Y). Tracking time interval is 8 minutes/frame, with a total duration of 800 minutes.

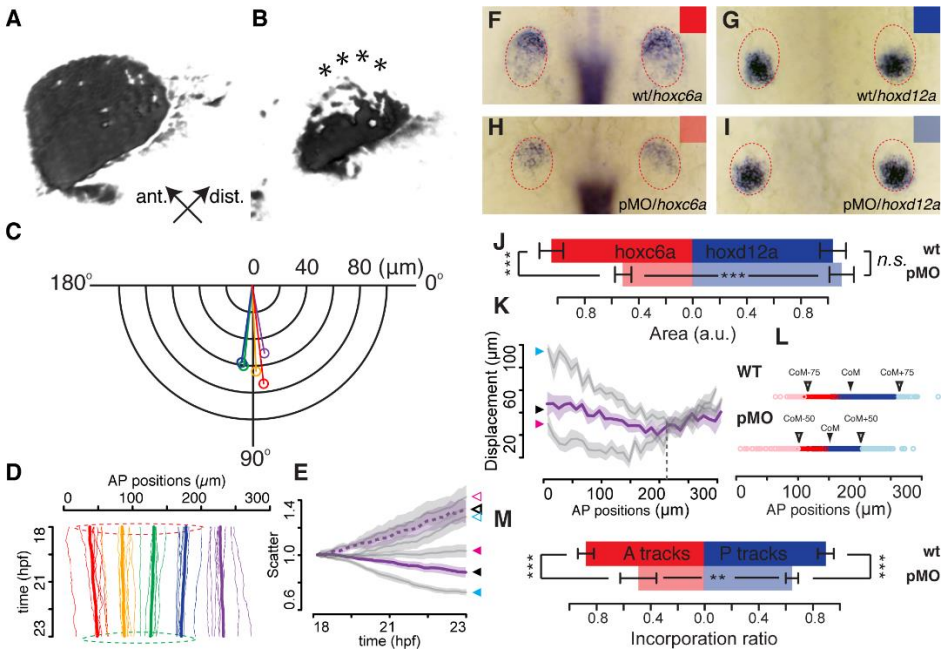

Figure S6 (related to Figure 6). Incomplete cell convergence in the limb field of Fgf24 partial morphants correlates with observed anteriorly biased truncations in limb AP axis.
A, B) Maximum intensity projections of the pectoral fin cartilaginous disc in a wildtype A) and an Fgf24 partial morphant B) 4 dpf larva. Arrows in A) show anterior and distal directions in A, B). Asterisks in B) highlight lesions on the anterior edge of the cartilaginous disc.
C) Polar plot showing the average orientation and magnitude of 2D displacement in 5 track groups subtracted by the average displacement of all LPM tracks in 8 Fgf24 partial morphant embryos.
D) Average net AP trajectories of 5 track groups subtracted by the average trajectories in all LPM tracks in 8 Fgf24 partial morphant embryos. Dotted circles highlight the similar sizes in limb field domains between tracks start (red) and end (green).
E) Scatter value along the AP axis plotted against time in 8 wildtype (blue arrowhead), 8 Fgf24 full Morphants (pink arrowhead), and 8 Fgf24 partial morphants (black arrowhead). Solid arrowhead: limb field. Open arrowhead: peritoneum field. Lines represent 8-embryo average; shaded areas represent 8-embryo standard error.
F-I) Expression patterns of *hoxc6a* (F, H) and *hoxd12a* (G, I) in 36 hpf limb buds of wildtype F, G) and Fgf24 partial morphant embryos H, I) (dorsal view, anterior up).
J) Quantification of expression areas of *hoxc6a* (red) and *hoxd12a* (blue) in wildtype (dark color) and Fgf24 partial morphants (light color) (n = 40 each). Wilcoxon test: p (hoxc6a wildtype-Fgf24 pMO) = 1.2×10^{-13} (***), p (hoxd12a wildtype-Fgf24 pMO) = 0.3, p (hoxc6a Fgf24 pMO-hoxd12a Fgf24 pMO) = 2.2×10^{-16} (***).
K) AP Displacement plotted against track start AP positions in 8 wildtype (blue arrowhead), 8 Fgf24 full morphants (green arrowhead), and 8 Fgf24 partial morphants (black arrowhead). Dotted vertical line represents the rough boundary at somite 4/5 between the limb field and the peritoneum field. Solid lines represent 8-embryo average; shaded areas represent 8-embryo standard error.

L) Track end AP positions of limb field tracks in 8 wildtype (wildtype) and 8 Fgf24 partial morphants (pMO). CoM: center of mass. CoM-75/CoM+75: anterior/posterior limits of the wildtype limb bud. CoM-34/CoM+34: anterior/posterior limits of the Fgf24 partial morphant limb bud.
M) Quantification of incorporation ratio of anterior (red, somites 1-2) and posterior (blue, somites 3-4) limb field tracks in wildtype (dark color) and Fgf24 partial morphants (light color) (n = 40 each). Wilcoxon test: p (A tracks wildtype-Fgf24 pMO) = 3.1×10^{-4} (***), p(P tracks wildtype-Fgf24 pMO) = 1.6×10^{-4} (***), p (A tracks Fgf24 pMO-P tracks Fgf24 pMO) = 0.02813 (*).

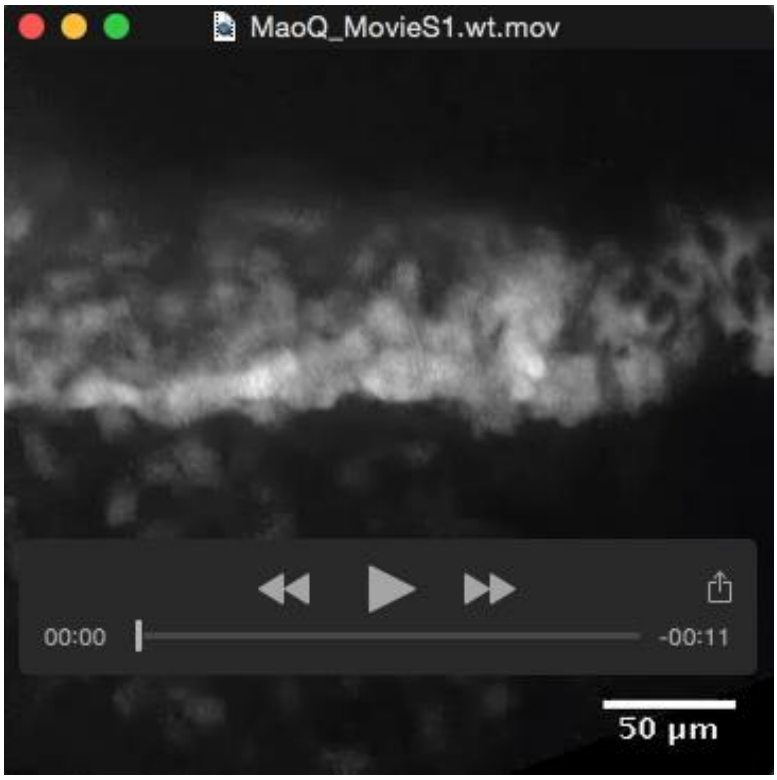

Movie 1 (related to Figure 2). Asymmetric and spatiotopic convergence of limb field LPM cells in a wildtype embryo. Time-lapse movie of a wildtype *Et(hand2:eGFP)ch2*; *Tg(h2afx:h2afv-mCherry)mw3* embryo, as shown in Figure 2A/A'~D/D'. Time interval: 8 min.

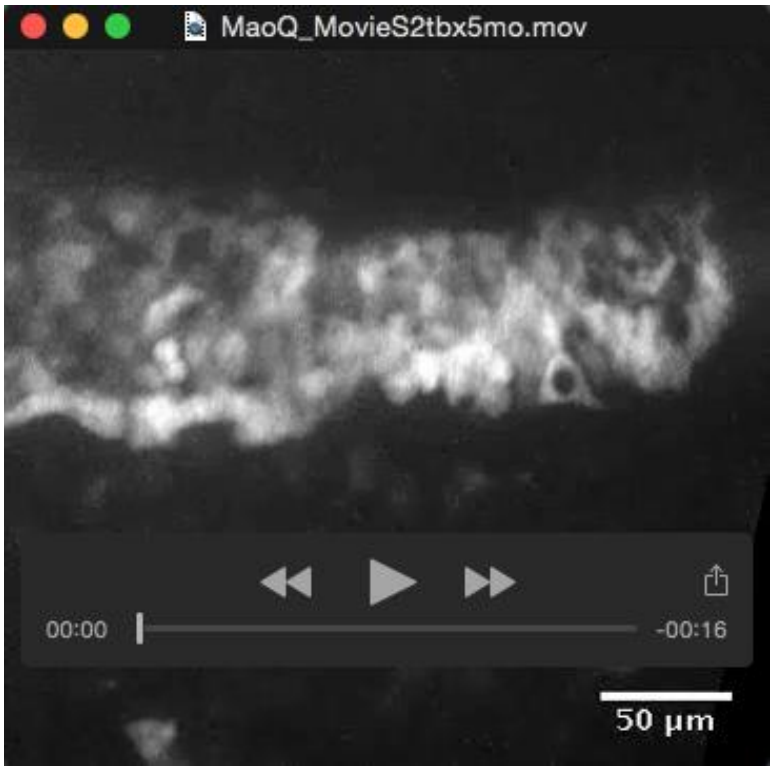

Movie 2 (related to Figure 3). Lack of convergence, but maintenance of migration spatiotopicity, in limb field LPM cells in a Tbx5a full morphant embryo. Time-lapse movie of a Tbx5a full morphant *Et(hand2:eGFP)ch2*; *Tg(h2afx:h2afv-mCherry)mw3* embryo, as shown in Figure 3A/A'~D/D'. Time interval: 8 min.

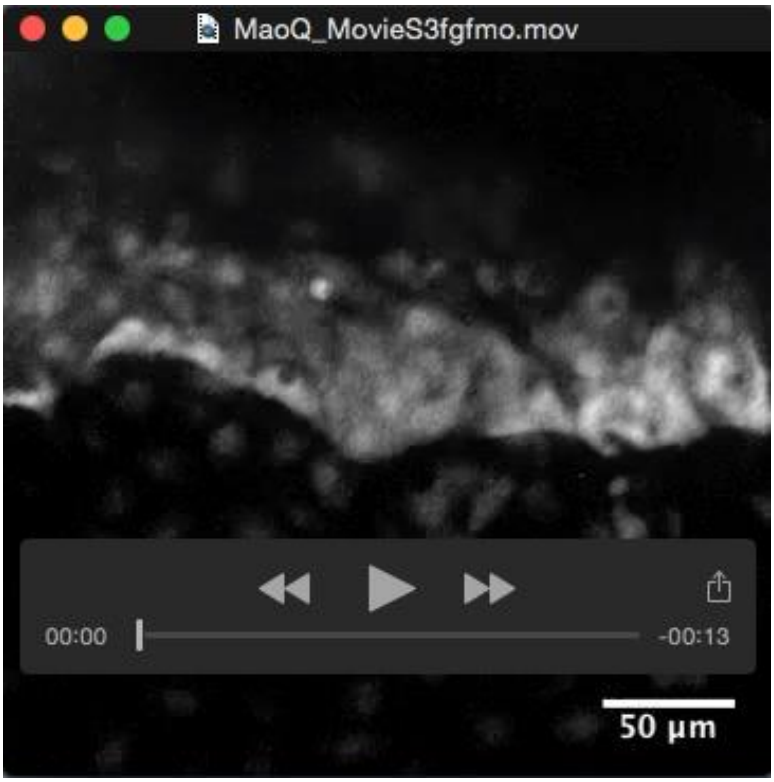

Movie 3 (related to Figure 4). Lack of convergence, but maintenance of migration spatiotopicity, in limb field LPM cells in an Fgf24 full morphant embryo. Time-lapse movie of a Fgf24 full morphant *Et(hand2:eGFP)ch2*; *Tg(h2afx:h2afv-mCherry)mw3* embryo, as shown in Figure 4A/A'~D/D'. Time interval: 8 min.

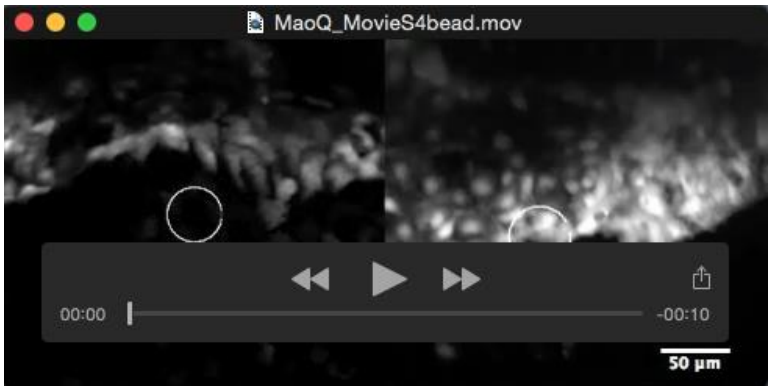

Movie 4 (related to Figure 5). Convergence of limb field LPM cells towards an Fgf source. Time-lapse movie of a Fgf24 full morphant *Et(hand2:eGFP)ch2*; *Tg(h2afx:h2afv-mCherry)mw3* embryo with a BSA (A) or Fgf8b (B)-coated bead (heighted in a white circle). Time interval: 8 min.

SUPPLEMENTAL EXPERIMENTAL PROCEDURES

Generation of Et(hand2:eGFP)ch2

Et(hand2:eGFP)ch2 (D.G. Ahn, University of Chicago, present address: Department of Biology, Chungnam National University, Daejeon, Republic of Korea) was recovered from a Tol2 enhancer trap screen based on eGFP expression pattern and outcrossed to *AB wildtype individuals for more than three generations to ensure the observed eGFP expression pattern was associated with a single-insertion site. The Tol2 transposon plasmid used for this screen, pT2KXIGΔ, is as described in (Urasaki et al., 2006). The transposon insertion site in *Et(hand2:eGFP)ch2* is mapped at the 5' UTR of *hand2* with the PCR-based Universal Fast Walking method, as described in (Myrick and Gelbart, 2002), then further confirmed with regular PCR (Figure S1). *Et(hand2:eGFP)ch2* is maintained and used as hemizygotes to control for any potential deleterious effects of the transgenic insertion.

Morpholinos

The antisense oligonucleotide (morpholino) used in this study against *tbx5a* (5'-CCTGTACGATGTCTACCGTGAGGC-3') is as described in (Ahn et al., 2002). The dose of morpholino per injection is measured following the protocol recommended by Gene Tools, LLC. The morpholino concentration is titrated such that we achieve 100% pectoral fin absence using the lowest possible dose, which was determined to be 1 ng per embryo for our anti-*tbx5a* morpholino.

mRNA *in situ* hybridization and immunochemistry

DIG-labeled antisense riboprobe were generated based on *tbx5a*, *hand2*, and *egfp* mRNA sequences (Roche Applied Science). Chromogenic antibody staining was performed as described in (Skromne et al., 2007) with the following modifications: primary mouse anti-myosin heavy chain antibody (A4.1025, Developmental Studies, Hybridoma Bank, IA, USA) was used at a dilution of 1:100; secondary peroxidase-labeled anti-mouse IgG (H+L) antibody (Vector laboratories, PI-2000) was use at a dilution of 1:200. DAB color product was developed with the Peroxidase Substrate Kit (Vector laboratories, SK-4100).

Trajectory analyses

The final tracking dataset contains the following parameters: AP position (x), ML position (y), time (t) and track serial (tr). From these four variables, we further calculated the following variables: Scatter, Displacement, Instantaneous Speed, Average Speed, Persistence, MSD, and Similarity between nearest neighbors. The mathematical definition for each variable is listed as follows. All calculation and data visualization were performed using R software (Team).

Scatter. Scatter is defined as the standard deviation of x (or y) of a given group of points at a given time point (t = i), divided by the standard deviation of x (or y) of the same group of points at the starting point (t = 1) (formula 1a for x, formula 1b for y). Therefore, Scatter is a measure of the fold change of "scattering" of a group of spots compared to their starting positions. Scatter is expressed either as a function of time, or as a function of AP positions:

$$Scatter.x(x=i,t=j)=\frac{\sigma(x_{x=1:i,t=j})}{\sigma(x_{x=1:i,t=1})} \quad (1a)$$

$$Scatter.y(x=i,t=j)=\frac{\sigma(y_{x=1:i,t=j})}{\sigma(y_{x=1:i,t=1})} \quad (1b)$$

The Scatter value along the AP axis (Scatter x) is used to partition the limb field and the peritoneum field. As shown in Figure S4, as the posterior limit of track groups used for calculating Scatter x expands posteriorly, Scatter x value at 23 hpf drops to the lowest at around 200 μm along the AP axis (roughly correlated with the boundary between somite 4~5), suggesting that cells posterior to this position (peritoneum) fail to converge with more anterior cells (limb field).

Displacement. Displacement is defined as the overall change of x (or y) of a given track spot between the start (t = 1) and the end of the track (t = 40) (formula 2a for x, formula 2b for y). Displacement is expressed as a function of track origin:

$$Displacement\_x(x,t=1) = x_{x,t=40} - x_{x,t=1} \qquad (2a)$$

$$Displacement\_y(x,t=1) = y_{x,t=40} - y_{x,t=1} \qquad (2b)$$

Speed. Instantaneous Speed is defined as the change of *x* (or *y*) of a given track spot between two consecutive time points (formula 3a for *x*, formula 3b for *y*). ***Average Speed*** is the mean of Instantaneous Speed for a given track spot across all time points.

$$Inst\_speed\_x(x,t=i) = x_{x,t=i+1} - x_{x,t=i} \qquad (3a)$$

$$Inst\_speed\_y(x,t=i) = y_{x,t=i+1} - y_{x,t=i} \qquad (3b)$$

$$Ave\_speed\_x(x) = \frac{1}{39}\sum_{i=1}^{40}(x_{x,t=i+1} - x_{x,t=i}) \qquad (4a)$$

$$Ave\_speed\_y(x) = \frac{1}{39}\sum_{i=1}^{40}(y_{x,t=i+1} - y_{x,t=i}) \qquad (4b)$$

Persistence. Persistence is defined as the ratio of Displacement over the overall trajectory length for a given track along the AP or ML axis (formula 5a for *x*, formula 5b for *y*). Persistence roughly describes the efficiency of cell migration along a given direction (Persistence = 1 means the cell migrates in a straight line, Persistence = 0 means the cell returns to its original position). However, Persistence is limited by that it does not consider the intermediate migration process, and thus cannot distinguish between, for example, random walk or back-and-forth directional movement. This limitation can be resolved by calculating MSD.

$$Persistence\_x(x) = \frac{x_{x,t=40} - x_{x,t=1}}{\sum_{i=1}^{40}(x_{x,t=i+1} - x_{x,t=i})} \qquad (5a)$$

$$Persistence\_y(x) = \frac{y_{x,t=40} - y_{x,t=1}}{\sum_{i=1}^{40}(y_{x,t=i+1} - y_{x,t=i})} \qquad (5b)$$

MSD (Mean Square Displacement). The formula for MSD is described in 6a (for *x*) and 6b (for *y*). N represents total number of time points. n represents current number of time points since the starting point. Δt represents the interval between two consecutive time points. The shape of the MSD~n function (equals MSD~t) describes the mode of migration, as MSD increases linearly with time during random walk, and quadraticly with time in directional migration (Berg, 1993; Codling et al., 2008). Thus on the logarithmic scale, MSD~time function has a slope of 1 during random walk, and 2 during directional migration.

$$MSD.x(n) = \frac{1}{N-n}\sum_{i=1}^{N-n}[x_{(n+i)\Delta t} - x_{i\Delta t}]^2 \qquad (6a)$$

$$MSD.y(n) = \frac{1}{N-n}\sum_{i=1}^{N-n}[y_{(n+i)\Delta t} - y_{i\Delta t}]^2 \qquad (6b)$$

MSD increases linearly with time during a random walk, but quadratically with time during directional migration bouts (Berg, 1993; Codling et al., 2008). Figure S3F shows that tracking groups 1 (red) and, to a lesser extent, tracking group 2 (yellow) exhibit significantly higher MSD values over time compared to other tracking groups, indicating a higher degree of directional migration exhibited by these anterior LPM cells. We further quantified the slope value in linear model log(MSD)~time. A slope for log(MSD)~time equaling 1 suggests random walk, whereas a slope equaling 2 is indicative of directional migration. We observed an the elevated slope value in linear model log(MSD)~time between track group 1 and the rest of limb field cells (Figure S3G), suggesting a more directional motion pattern in track group 1 cells. Strikingly, in full or partial morphants for Tbx5a or Fgf24, this anterior elevation of AP cell motility, as measured by Displacement, Average Speed, Persistence and MSD, is lost or diminished (Figure 3J, Figure 4K, Figure S3A1-D1, A2-D2). This suggests that Tbx5a and Fgf24 are required for the directional convergent motility of the anterior-most LPM cells along the AP axis. Same sets of measurements along the orthogonal axis (mediolateral axis, ML) are also presented (Figure S3C-E, H-J). Interestingly, we observed a descending trend of ML motility along the AP axis in Fgf24 full morphants (Figure S3C-E, third column), reminiscent of the descending trend of ML motility along the AP axis in wildtype embryos. This might reflect a redirection of cell motility in the anterior-most LPM cells from caudal-oriented to lateral-oriented upon loss of the convergent cue Fgf24.

Similarity. The motion similarity between nearest neighbors i and j is defined as the cosine value of the angle formed between their instantaneous velocities. Similarity can be expressed as a function of time or nearest neighbor pairs. In the case of independent random walk, the histogram of similarity is symmetrical on either side of 0 degree, representing equal probability of two nearest neighbors going parallel or anti-parallel.

$$Similarity_{ij}(t) = \cos(\arctan(\frac{y_{i,t+1} - y_{i,t}}{x_{i,t+1} - x_{i,t}}) - \arctan(\frac{y_{j,t+1} - y_{j,t}}{x_{j,t+1} - x_{j,t}})) \quad (7)$$

Center of Mass and defining the limb bud region. The wildtype limb bud region is defined as the region within ±75 μm to the average end positions of all limb field tracks (**Center of Mass**). The expression area of *hoxc6a* and *hoxd12a* in wildtype and Tbx5a partial morphants indicates that the size of limb bud in Tbx5a partial morphants is roughly 45% of the wildtype limb bud size. The Tbx5a partial morphant limb bud region is thus defined as the region within ±34 μm to the average end positions of all limb field tracks.

Incorporation ratio. The Incorporation ratio is defined as the ratio of tracks from a given AP region that end up in the limb bud region over all tracks from the same AP region. For

instance, the Incorporation ratio of anterior limb field tracks are defined as all tracks that are from the anterior limb field (from somite levels 1 and 2) that ends up in the limb bud region divided by all tracks from the anterior limb field. The Incorporation ratio of posterior limb field tracks are defined as all tracks that are from the posterior limb field (from somite levels 3 and 4) that ends up in the limb bud region divided by all tracks from the posterior limb field.

Simulation of a 2D random walk population

The highly spatiotopic LPM cell migration lead us to speculate that this might be a form of collective cell migration (Friedl and Gilmour, 2009; Rørth, 2009). To investigate whether individual LPM cells are constrained in their motility, we compared the observed LPM cell motility with that from a simulated 2D random walking population (Figure S4). We first compared the correlation between the start and the end positions between the observed conditions (Figure S4B-F) and the simulated condition (Figure S4A). While the coefficient of determination (R^2) is comparable between all experimental conditions (Figure S4B-F), it is much lower in the simulated 2D random walk population (Figure S4A), indicating LPM cell migration has higher spatiotopicity than would be seen if cells were undergoing a random walk. We then tested if the angles between the instantaneous velocities of nearest neighbors are comparable in all conditions. In the Similarity histogram, we observed a strong bias towards smaller angles (Similarity close to 1) in wildtype, Tbx5a full morphants and Tbx5a partial morphants, in contrast to the symmetrical distribution in the 2D random walk population (Figure S4E, Kolmogorov-Smirnov Test: Simulated~WT: $p < 2.2 \times 10^{-16}$). This indicates certain similarity and thus coordination in motility directions between nearest neighbors in all experimental conditions.

The 2D random walk population was simulated in the following steps:

1) Assign the start positions of the population the identical start positions of the wildtype population;
2) For each instantaneous migration step, assign instantaneous speeds randomly chosen from distributions with parameters comparable to the observed corresponding values in the wildtype dataset, and angles randomly chosen from a uniform distribution of [0, pi] (assuming LPM cells do not cross the midline).

SUPPLEMENTAL REFERENCES

Ahn, D.-G., Kourakis, M.J., Rohde, L.A., Silver, L.M., and Ho, R.K. (2002). T-box gene tbx5 is essential for formation of the pectoral limb bud. Nature *417*, 754–758.

Berg, H. (1993). Random Walks in Biology (Princeton University Press).

Codling, E.A., Plank, M.J., and Benhamou, S. (2008). Random walk models in biology. J R Soc Interface *5*, 813–834.

Friedl, P., and Gilmour, D. (2009). Collective cell migration in morphogenesis, regeneration and cancer. Nat Rev Mol Cell Biol *10*, 445–457.

Myrick, K.V., and Gelbart, W.M. (2002). Universal Fast Walking for direct and versatile determination of flanking sequence. Gene *284*, 125–131.

Rousseeuw, P.J., and Leroy, A.M. (2005). Robust Regression and Outlier Detection (Wiley).

Rørth, P. (2009). Collective cell migration. Annu Rev Cell Dev Biol *25*, 407–429.

Skromne, I., Thorsen, D., Hale, M., Prince, V.E., and Ho, R.K. (2007). Repression of the hindbrain developmental program by Cdx factors is required for the specification of the vertebrate spinal cord. Development *134*, 2147–2158.

Team, R.C. R: A language and environment for statistical computing. www.R-Project.org.

Urasaki, A., Morvan, G., and Kawakami, K. (2006). Functional Dissection of the Tol2 Transposable Element Identified the Minimal cis-Sequence and a Highly Repetitive Sequence in the Subterminal Region Essential for Transposition. Genetics *174*, 639–649.